

NASA-TM-112525

BROADBAND HIGH-ENERGY OBSERVATIONS OF THE SUPERLUMINAL JET SOURCE GRO J1655–40 DURING AN OUTBURST

S. N. ZHANG,^{1,2} K. EBISAWA,^{2,3} R. SUNYAEV,⁴ Y. UEDA,⁵ B. A. HARMON,¹ S. SAZONOV,⁴
 G. J. FISHMAN,¹ H. INOUE,⁵ W. S. PACIESAS,^{1,6} AND T. TAKAHASHI⁵

Received 1996 July 31; accepted 1996 November 4

ABSTRACT

The X-ray/radio transient superluminal jet source GRO J1655–40 was recently suggested to contain a black hole from optical observations. Because it is a relatively close-by system ($d \sim 3.2$ kpc), it can likely provide us with rich information about the physics operating in both Galactic and extragalactic jet sources. We present the first simultaneous broadband high-energy observations of GRO J1655–40 during the 1995 July–August outburst by three instruments: *ASCA*, *WATCH/Granat*, and *BATSE/CGRO*, in the energy band from 1 keV to 2 MeV. Our observations strengthen the interpretation that GRO J1655–40 contains a black hole. We detected a two-component energy spectrum, commonly seen from other Galactic black hole binaries, but never detected from a neutron star system. Combining our results with the mass limits derived from optical radial velocity and orbital period measurements, we further constrain the mass of the central object to be between 3.3 and $5.8 M_{\odot}$, above the well-established mass upper limit of $3.2 M_{\odot}$ for a neutron star (the optical mass function for GRO J1655–40 is $3.16 \pm 0.2 M_{\odot}$). This system is therefore the first Galactic superluminal jet source for which there is strong evidence that the system contains a stellar mass black hole. The inclination angle of the binary system is constrained to be between 76° and 87° , consistent with estimates obtained from optical light curves and radio jet kinematics.

Subject headings: binaries: close — black hole physics — gamma rays: observations — stars: individual (GRO J1655–40) — X-rays: stars

1. INTRODUCTION

Radio observations are now beginning to show that relativistic jets may be a more common feature of X-ray binary systems than previously thought. Some, such as SS 433 (Margon 1988), Cygnus X-3 (Strom et al. 1989), and the more recently discovered superluminal transients GRS 1915+105 (Mirabel & Rodríguez 1994) and GRO J1655–40 (Tingay et al. 1995; Hjellming & Rupen 1995) show proper motions implying velocities $V \sim 0.2$ – $0.9c$. Of those, only GRO J1655–40 has a compact object whose dynamically estimated mass is greater than $3 M_{\odot}$ (Bailyn et al. 1995b). *It is thus generally believed to be a black hole binary (BHB).* Because it is a BHB with relativistic jet ejection episodes, GRO J1655–40 is a good analog to the active galactic nuclei (AGNs), which are thought to contain supermassive black holes and frequently are observed to have relativistic jets associated with the central engine.

The Galactic jet sources are of great interest because the dynamic timescales of BHBs are a factor of $\sim 10^6$ – 10^9 smaller than those of typical AGNs (Shakura & Sunyaev 1976). Therefore, dynamical variations of AGNs on timescales from many years up to the Hubble time correspond in BHBs to intervals of seconds to years. Observations of jet

formations and decay in coincidence with studies of overall flux variations and spectral evolution allow the possibility of identifying the emission regions at various wavelengths.

Studying the inner part of the accretion disk very close to the central black hole is critical for understanding the central engine and the jet ejection. This region can be observed at X-ray and hard X-ray wavelengths for BHBs. For AGNs, however, this region is much more difficult to observe. This is because the typical photon energy radiated from the inner accretion disk region of an AGN is much lower (\sim eV). Absorption of such low-energy photons in the complex surrounding environment and the interstellar medium is severe. Thus GRO J1655–40 is a unique system for understanding the physics involved in accreting black holes and relativistic jets in our own Galaxy and AGNs.

Since the discovery of GRO J1655–40 (Zhang et al. 1994a) by the Burst and Transient Source Experiment (BATSE) aboard the NASA *Compton Gamma-Ray Observatory* (CGRO) on 1994 July 27, it has been extensively observed in radio, optical, X-ray, and gamma-ray bands. Radio observations have revealed several relativistic ejection episodes (Tingay et al. 1995; Hjellming & Rupen 1995) from this system, following hard X-ray (above 20 keV) activity (Harmon et al. 1995). Optical observations (Bailyn et al. 1995a, 1995b) have determined the orbital period (2.62 days), the nature of the companion star (F-type), and the mass limit of the central compact object ($\geq 3 M_{\odot}$).

The BATSE experiment detected four major outbursts from this system separated by about 120 days (Zhang et al. 1995a). Two of them were also observed by the WATCH instrument on the *Granat* satellite (Sazonov, Sunyaev, & Lund 1996). The energy spectrum above 20 keV when the

¹ ES-84, NASA/Marshall Space Flight Center, Huntsville, AL 35812.

² Universities Space Research Association.

³ Code 660.2, NASA/Goddard Space Flight Center, Greenbelt, MD 20771.

⁴ Space Research Institute, Moscow, Russia; and Max-Planck-Institut für Astrophysik, Garching, Germany.

⁵ Institute of Space and Astronautical Science, Kanagawa, Japan.

⁶ University of Alabama in Huntsville, Huntsville, Alabama.

source is in outburst is well described by a power law (photon index 1.5–3.1) up to at least 200 keV. OSSE/CGRO detected emission up to 600 keV without any detectable deviation from the power law (Kroeger et al. 1996). Searches in both BATSE and OSSE data for rapid variability resulted in upper limits of about 5% of integrated rms noise from 0.01 to 1 Hz (Kroeger et al. 1996; Crary et al. 1996). In light of the possible optical eclipses (Bailyn et al. 1995a; but cf. van der Hooft et al. 1996), both BATSE and OSSE data were searched for orbital eclipses and/or modulation. No indications of periodic behavior were found (Zhang et al. 1997; Kroeger et al. 1996).

The TTM instrument (2–27 keV) aboard the Russian *Mir* space station also observed this source on several occasions (1994 September and October and 1995 February) between the main hard X-ray outbursts detected by BATSE. An ultrasoft spectrum, compatible with an accretion disk origin, was observed during most of these observations (Alexandrovich et al. 1994; Alexandrovich, Borozdin, & Sunyaev 1995). Sometimes a hard X-ray tail was seen by TTM and HEXE (15–200 keV) also aboard the *Mir* station (Sunyaev et al. 1997). X-ray observations of GRO J1655–40 in the 1–10 keV range with the Japanese ASCA satellite have revealed very unusual spectral characteristics. On two occasions, 1994 August 23 and September 27, when the source flux in the BATSE energy band (20–100 keV) was very low (<30–50 mCrab), ASCA detected an energy spectrum with a significant high-energy cutoff above 4–5 keV. Absorption-line features were seen in the region of the Fe K-edge (Ueda et al. 1997).

2. MULTI-INSTRUMENT OBSERVATIONS

The outburst in 1995 July–August was simultaneously observed from 1 keV to 2 MeV by ASCA (1–10 keV), WATCH/Granat (8–20 keV), and BATSE/CGRO (20–2000 keV) instruments. The X-ray telescope (Tanaka, Inoue, & Holt 1994) aboard the Japanese satellite ASCA uses focusing X-ray optics to concentrate X-ray photons in the 1–10 keV range onto its detector planes, the solid state spectrometer (SIS), and the gas imaging spectrometer (GIS). The SIS was not usable for this observation owing to the brightness of the source, which caused telemetry saturation and pulse pile-up. The GIS was usable for energy spectral measurements, though significant dead time was present. Dead time was corrected for in estimating the incident source flux. The ASCA observation occurred between 1995 August 15.45 and 16.18 (UT), during the rise to the second peak of this outburst. Overall flux variations during the nearly 1 day observation were less than 10%.

The WATCH instrument (Lund 1986) aboard the Russian *Granat* spacecraft detected this outburst while the *Granat* Observatory was scanning the sky. In the scanning mode, the motors of the WATCH collimators do not rotate, and the spinning of the satellite is used to produce modulation patterns. A detailed analysis of the data was done to separate the contributions of GRO J1655–40 and the nearby source 4U 1700–37 to the modulation curve. Observations during the X-ray eclipses of 4U 1700–37 and simulations of the instruments' imaging capability gave proof that the obtained light curve of GRO J1655–40 is correct.

GRO J1655–40 has been continuously monitored by BATSE's Large Area Detectors (LADs) (Fishman et al. 1989) using Earth occultation analysis (Harmon et al. 1992)

and Earth occultation transform imaging (Zhang et al. 1993, 1994b, 1995b) techniques. The uncollimated nature of the LADs makes other active sources also detectable during these outbursts. The data are thus simultaneously fitted with these sources included to determine the net contributions from GRO J1655–40.

3. BROAD ENERGY BAND SPECTRUM

The ASCA-BATSE measured spectrum is shown in Figure 1. The ASCA data cannot be fitted by standard single-component models. However, they are consistent with a two-component spectral model, consisting of a power-law component and a multicolor blackbody disk (MCBD) component (Shakura & Sunyaev 1973; see Mitsuda et al. 1984 and Makishima et al. 1986 for the MCBD model). The flux detected by WATCH in the 8–20 keV range during this time was 620 ± 50 mCrab (here the Crab flux was determined contemporaneously with the GRO J1655–40 observation). The WATCH detection is also plotted in the same figure. Extrapolation of the BATSE power-law spectrum into the WATCH energy range gives ~ 240 mCrab. The WATCH flux thus independently suggests the presence of some additional soft component, which should contribute ~ 380 mCrab in the 8–20 keV flux. The ultrasoft component observed with ASCA fitted by the MCBD model would produce ~ 400 mCrab in the WATCH energy band; therefore, the value of the flux measured with WATCH is in a good agreement with a model consisting of a power-law component and a MCBD component. No other spectral component is needed to account for the 1–200 keV overall spectrum, except for a weak absorption feature in the Fe K-fluorescence energy band of the ASCA data (Ueda et al. 1997). The ASCA continuum model parameters for this two-component spectrum are as

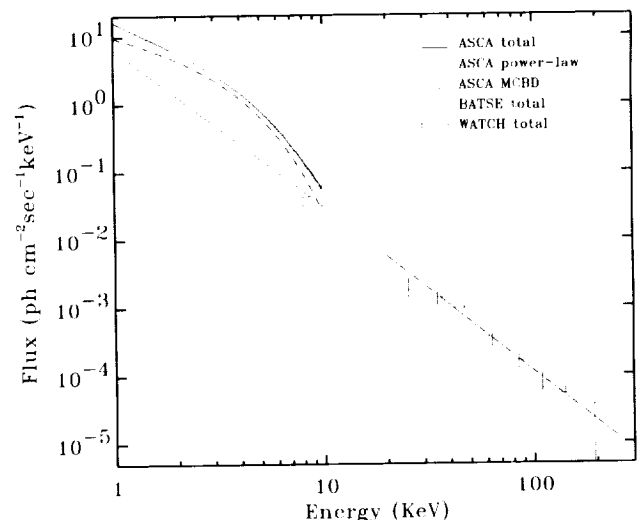


FIG. 1.—Joint ASCA/BATSE spectrum with WATCH integrated flux for 1995 August 15–16. Spectral models and data points are shown (ASCA error bars are extremely small). The total ASCA energy spectrum is composed of two components, i.e., an ultrasoft component described by a multicolor blackbody disk (MCBD) model and a power-law component that is consistent, when extrapolated into the BATSE energy range, in both photon index and flux with the independently determined BATSE power law. The WATCH data point is consistent with the sum of these two components. No third spectral component is required for the entire 1–100 keV spectrum, except for a weak absorption-line feature in the iron K-fluorescence energy band of the ASCA data.

follows: neutral hydrogen column density $N_H = (8.9 \pm 0.3) \times 10^{21} \text{ cm}^{-2}$; inner disk edge temperature $kT_{\text{in}} = 1.36 \pm 0.01 \text{ keV}$; inner disk radius $R_{\text{in}}[\cos(i)]^{1/2} = 9.3 \pm 0.2 \text{ km}$ (at 3.2 kpc), where i is the inclination angle of the system; power-law photon spectral index $\alpha = 2.36 \pm 0.08$ and the normalization factor $a_0 = 6.3 \pm 0.9 \text{ photons s}^{-1} \text{ cm}^{-2} \text{ keV}^{-1}$ at 1 keV for the power law. The independently determined BATSE power-law parameters are as follows: photon spectral index $\alpha = 2.43 \pm 0.3$ and flux $1.05 \times 10^{-3} \pm 1.7 \times 10^{-4} \text{ photons s}^{-1} \text{ cm}^{-2} \text{ keV}^{-1}$ at 40 keV. The *ASCA* and BATSE power laws are consistent with each other within their statistical errors.

4. SOURCE INTENSITY VARIABILITY

Source intensity variations on timescales of seconds to hundreds of seconds can be studied with both *ASCA* and BATSE. Telemetry saturation and dead time make it impossible to study short-term variations using the *ASCA* GIS event data that we used to obtain the energy spectrum discussed in the last section. However, the GIS monitor counter (type "L1"), which has neither position nor energy resolution, is usable for short-term variation studies. All the GIS events that passed the pulse-height (0.9–10 keV) and rise-time discriminators are recorded as monitor counts with a time resolution of 0.125 s. In Figure 2, we show a power density spectrum (PDS) of GRO J1655-40 calculated from the GIS monitor counts in the 0.002–4 Hz band, together with those of two black hole candidates (BHCs),

Cyg X-1 in a low state and the X-ray nova GRS 1009-45 in a high state (Sunyaev et al. 1994) for comparison. The Poisson noise level has been subtracted. The GRO J1655-40 PDS clearly shows excess power above the law, $f^{-1.2}$. The rms variation relative to the average flux is $5.5\% \pm 0.2\%$. For comparison, the rms fraction for Cyg X-1 is $31.4\% \pm 0.3\%$. Significant short-term variations were not found from GRS 1009-45 in excess of the Poisson noise level.

The continuous counting rates of the BATSE LADs at a time resolution of 1.024 s were also analyzed for evidence of variability. The 20–100 keV flux, however, showed no variation at an upper limit of about 20% integrated from 0.01 to 0.488 Hz (D. Cray 1996, private communication). A smaller upper limit ($\sim 5\%$) was obtained for other brighter outbursts from this source (Crary et al. 1996).

5. LIGHT CURVES AND SPECTRAL VARIATIONS

In Figure 3, we show the WATCH (8–20 keV) and BATSE (20–100 keV) light curves and spectral variations during the 1995 July–August outburst. The double-peak structure and overall spectral evolution are similar to that of the previous three major outbursts from this source (Zhang et al. 1997). It is interesting to compare the BATSE and WATCH measurements throughout the entire outburst. In Figure 3 (*upper panel*), we also plot the extrapolated BATSE flux in the 8–20 keV band from the measured fluxes in 20–100 keV band, together with the WATCH light

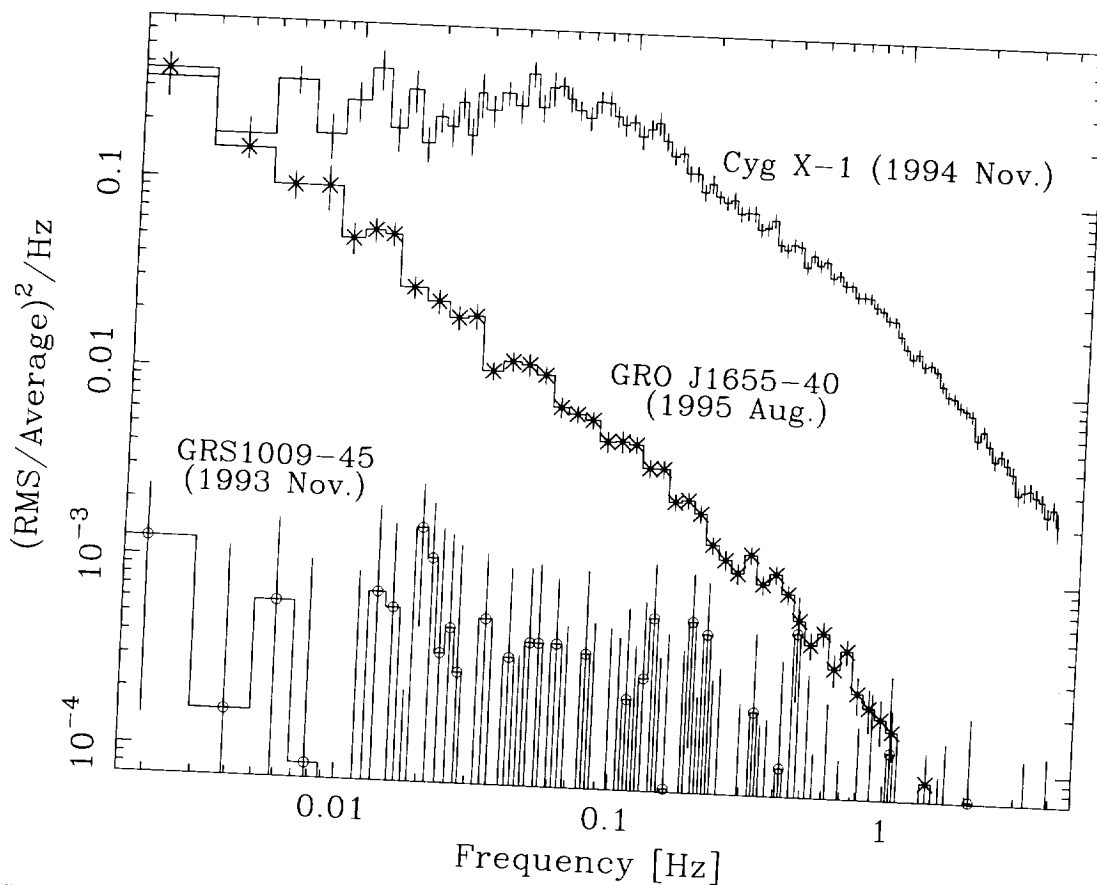


FIG. 2.—Normalized power density spectra of GRO J1655-40, Cyg X-1, and GRS 1009-45, obtained with the *ASCA* GIS monitor. The two BHCs, Cyg X-1 and GRS 1009-45, were in a typical low state and high state, respectively. The power-law PDS of GRO J1655-40 is very unusual among BHCs.

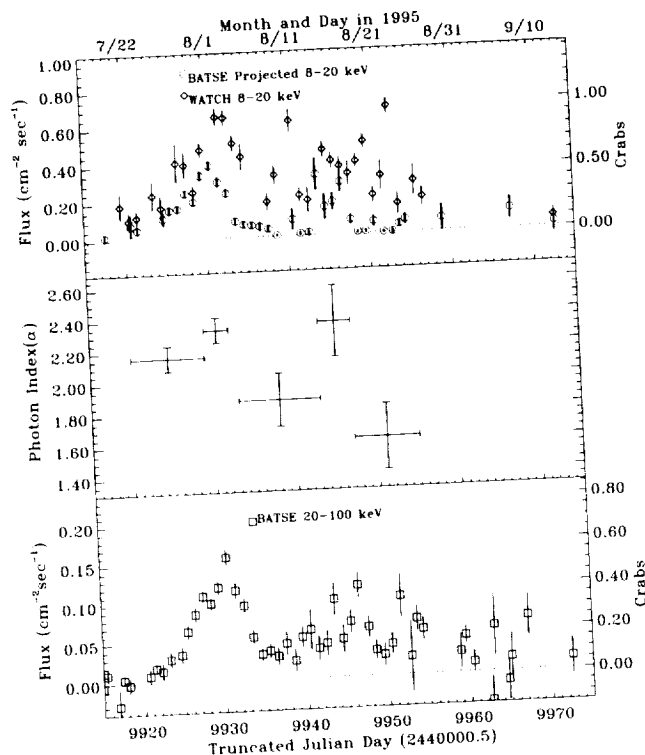


FIG. 3.—BATSE and WATCH light curves and spectral variations. The top panel displays the WATCH 8–20 keV light curve (diamonds) and the projected flux in 8–20 keV from power-law fits to the 20–100 keV BATSE total spectra (circles). The spectral index was allowed to vary. The total 8–20 keV fluxes detected by WATCH are always above the 20–100 keV power-law extrapolation, which indicates the existence of an additional soft component. The middle panel shows the photon spectral index of the 20–100 keV power law observed by BATSE. The bottom panel is the BATSE light curve in the 20–100 keV band.

curve. The extrapolated BATSE 8–20 keV light curve should be dominated by the power-law component since any thermal component from the accretion disk cannot contribute significantly to the 20–100 keV band power law. It is clear that whenever the source was simultaneously detected by both WATCH and BATSE, the WATCH flux level is almost always significantly above the power-law component projected from BATSE measurements. The ASCA detection of the disk blackbody component suggests that all the additional flux observed by WATCH originates from the accretion disk. It is interesting to note that during TJD 9947–9956, the 8–20 keV flux is dominated by the thermal component, while the 20–100 keV power law is very hard (photon spectral index ~ 1.5 –2.0).

6. DISCUSSION

6.1. GRO J1655–40 as a Black Hole System

For the first time, we have detected a two-component energy spectrum from a Galactic superluminal jet source during a hard X-ray outburst. The thermal component fits well with the MCB model commonly used to describe the X-ray emission from an optically thick and geometrically thin accretion disk. Using the measured energy spectrum, we can further constrain the parameters of the binary system. From the MCB model fitting, the inner disk radius is constrained to be $R_{in}[\cos(i)]^{1/2} = 9.3 \pm 0.2$ km (assuming the source is at a distance of 3.2 kpc). From the relationship between the Schwarzschild radius R_s and the

inner disk radius R_{in} , $3R_s \approx (\frac{3}{5}) \times 0.8 \times R_{in} \times f^2$, we can obtain the relationship between the mass of the central compact object (M) and the inclination angle of the system (i). In the above equation, the factor $\frac{3}{5}$ accounts for the disk effective temperature becoming a maximum at $\sim 5R_s$, and 0.8 is the relativistic correction for gravity becoming effectively stronger than in the Newtonian case. The factor f is the ratio between the color temperature and the effective temperature and should be ~ 1.7 (see Shimura & Takahara 1995 for details).

In Figure 4, we plot the primary mass versus inclination (M – i) derived from optical (mass function of $3.16 \pm 0.2 M_\odot$; Bailyn et al. 1995b) and X-ray spectroscopic observations. For the X-ray M – i relationship, we also plot the lower and upper bounds derived from the 3σ error of 0.6 km for R_{in} $[\cos(i)]^{1/2}$ combined with the lower and upper limits of 3.0 and 3.5 kpc for the source distance (Hjellming & Rupen 1995). A larger distance shifts the curve upward. The allowed parameter space is shown on the figure as the shaded area. We find the mass of the compact object lies between 3.3 and $5.8 M_\odot$ for all possible parameters. This lower mass limit is solidly above the well-established neutron star mass upper limit. The range of the inclination angle is between 76° and 87° , which is consistent with the optical light-curve modulation (Bailyn et al. 1995a, 1995b; van der Hooft et al. 1996) and radio jet kinematics solutions (Hjellming & Rupen 1995). We therefore conclude that this superluminal jet source contains a black hole and has the highest inclination angle of all Galactic BHBs with well determined system parameters.

The allowed parameter space can be further divided into two areas, labeled as A and B. For a minimum possible

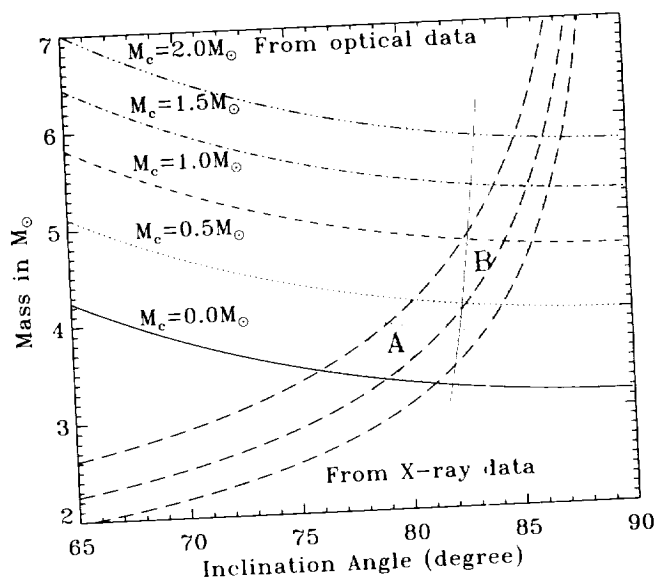


FIG. 4.—The relationships between the mass of the central compact object (black hole) and the binary system inclination angle in GRO 1655–40, as determined from optical radial velocity and X-ray spectroscopy measurements. The five nearly parallel and horizontal (thick) lines are from the optical radial velocity determination of the mass function (Bailyn et al. 1995b), corresponding to the companion mass of 0.0, 0.5, 1.0, 1.5, and $2.0 M_\odot$. The three nearly parallel curves from the lower left-hand corner to the upper right-hand corner are from the inner disk radius determined from X-ray spectroscopy. The allowed parameter space is indicated by two shaded areas: A (noneclipsing zone) and B (eclipsing zone), respectively (see text for details). The range of the compact object mass is constrained to be from 3.3 to $5.8 M_\odot$. The compact object is thus likely a black hole. The inclination angle of the binary system is between 76° and 87° .

companion mass of $0.1 M_{\odot}$ (below which such a binary system would not be formed), a sufficiently high inclination angle would result in the center of the accretion disk to be eclipsed by the companion. This “eclipse” line is depicted by the nearly vertical thin *solid* line. The parameter space on the right side of this line is a part of the *eclipsing zone*. For a lower inclination angle, a more massive companion will also result in such eclipse. The “eclipse” line corresponding to $0.32 M_{\odot}$ is shown as the vertical thin *dotted* line. The $0.32 M_{\odot}$ is chosen because this line intersects with the optical $M-i$ relationship for the same companion mass on the upper bound of the X-ray $M-i$. Therefore, if the system parameters fall in the area B, the accretion disk center will be eclipsed by the companion. In area A, no such eclipse will happen. The mass of the companion cannot be higher than $0.32 M_{\odot}$ for a noneclipsing system.

A reasonable mass of the companion is between 0.5 and $1.5 M_{\odot}$. In this case, this system will be the first detected eclipsing BHB in our Galaxy. Eclipse mapping may be applied to determine the details of the inner disk region for the first time. The BH mass lies between 4.1 and $5.3 M_{\odot}$, and the inclination angle is between 80° and 86.5° . The inner disk radius can be estimated to be between 25 and 36 km, considerably larger than that of neutron star binaries (~ 10 km). On the other hand, this system has an unusually large space velocity, which indicates that it probably has experienced an unusual evolution (Brandt, Podsiadlowski, & Sigurdsson 1995). Therefore, the companion could possibly be severely undermassive. Constraints from evolutionary theories suggest that the companion cannot be less massive than $0.23 M_{\odot}$ (Brandt et al. 1995). From Figure 4, it is clear that the allowed parameter space between 0.23 and $0.5 M_{\odot}$ companion is very small. This system may also be an important object for our understanding of the formation and evolution of BHBs.

Further support that the system contains a black hole is the lack of an additional thermal component commonly seen from a neutron star surface with a higher temperature (typically a ~ 2 keV blackbody spectrum, which is considerably harder than the MCB spectrum, i.e., the ultrasoft component). The ultrasoft component by itself, however, cannot be taken as a signature of a black hole, since 4U 0142+614, a neutron star pulsar system, has displayed such an ultrasoft spectrum (Mereghetti, Stella, & De Nile 1993; Israel, Mereghetti, & Stella 1993). Because of the mass accretion rate dependency of the disk temperature, a neutron star system may be observed with a very low disk temperature when its mass accretion rate is low and therefore the X-ray luminosity is low. We therefore argue that a *luminous* ($\sim 1 L_{\text{Eddington}}$ for $1 M_{\odot}$) *ultrasoft X-ray spectrum is a very strong indication of a black hole system* and should be used for selecting BHCs. A prominent power-law component associated with such a bright ultrasoft component, however, has never been observed from a neutron star system but is now seen from persistent, transient, and jet-type BHBs. *Such a two-component spectrum may, therefore, be a firm signature from a black hole system* (Sunyaev et al. 1988, 1994; van der Klis 1994; van der Klis & van Paradijs 1994; White 1993; Tanaka & Lewin 1995; Zhang et al. 1996).

6.2. Origin of the Power-Law Hard X-Ray Tail

We are reasonably confident that the ultrasoft component originates from the accretion disk owing to the

gravitational energy release of the accreted material in the X-ray energy band. The origin of the hard X-ray power-law component is, however, more controversial, although inverse-Compton upscattering of low-energy photons by fast-moving particles (electrons or protons) is commonly accepted as the radiation mechanism. The nondetection of short-term variations from the hard X-ray power-law component suggests a different origin of this power law than for the low-state hard X-ray power laws (with cutoff) observed from both black hole and neutron star binaries. Thermal Comptonization models normally used to interpret the low-state hard X-ray power laws cannot be applied here, regardless of the nature and geometries of the hot Compton cloud, because the relatively steep power law extended to a very high energy implies a very high electron temperature (50 – 200 keV) and a very small optical depth (0.01 – 0.1). It is very hard to keep this optically thin cloud sufficiently stable to account for the low (or no) short-term variability in the hard X-ray power-law component. Cooling of the high-energy electrons by the copious soft X-ray photons in the high state seems to be an additional complication, unless there is a powerful underlying heating mechanism.

Based on the detected relativistic jets from this source and the correlation of radio flares with hard X-ray activity, it has been suggested that the fast-moving particles responsible for the radio emission from the jets (Levinson & Blandford 1996) also scatter low-energy photons via the inverse-Compton process to produce the observed hard X-rays. We believe this is unlikely since this and the previous outburst were not detected to have any radio emission, unlike the first two outbursts with strong radio emission. The overall radio emission decayed exponentially since the initial hard X-ray outburst, while the hard X-ray outbursts with similar peak luminosities occurred 4 times since the initial outburst with a separation of about 120 days. Absence of the jet ejection and any radio emission at all during the last two hard X-ray outbursts argues strongly against the scenario in which hard X-rays are produced directly or indirectly from the jets.

The upper limit of about 0.5 mJy at 3.6 cm (Hjellming 1996) allows us to set a limit of the size of the possible radio emission region. The surface brightness (due to incoherent synchrotron radiation) temperature upper limit of 10^{12} K (Shu 1991) indicates that the dimension of the possible radio emission region is less than 1.7×10^{11} cm (R. M. Hjellming, private communication). This is smaller than the size of the binary system ($\sim 10^{12}$ cm) but can still be several orders of magnitude larger than the soft X-ray (blackbody) emission region ($\sim 10^7$ cm). Since this region is so close to and very likely covers completely the soft photon emission region, the high-energy electrons required for producing synchrotron radiations will be cooled down effectively by the inverse-Compton scattering process, thus preventing significant synchrotron radiations. Therefore, the power-law hard X-ray photons cannot be produced via the synchrotron radiation mechanism.

Another model involves the converging flow of fast-moving material near the black hole horizon (Chakrabarti & Titarchuk 1995). This model does not have the difficulties discussed above for other models. In this model, the power-law component is produced via the inverse-Compton scattering of low-energy photons of the ultrasoft component by the bulk motion of the converging flow. This model predicts a spectral break energy of ~ 511 keV divided by the total

mass accretion rate in terms of the Eddington rate corresponding to the central compact object mass. The detected luminosity during the *ASCA* observation is $\sim 10^{38}$ ergs s $^{-1}$ and could be a factor of 2–5 higher at other times (scaled up from the detected WATCH and BATSE fluxes). Therefore, the Eddington accretion rate is ≤ 1 for a 3–5 M_{\odot} black hole. The unbroken power law up to 200–600 keV is certainly consistent with this prediction. It is also interesting to note that a relativistic converging flow cannot take place near a neutron star surface when the mass accretion is high owing to the radiation pressure from the neutron star surface. *This provides a possible explanation why such a two-component spectrum has never been observed from a neutron star binary.* We consider, however, that it is still difficult within this model to explain the range of spectral variations during this outburst, especially the very hard power law with a huge thermal excess at low energies near the end of this outburst. If GRO J1655–40 were indeed an eclipsing system, this model would be excluded, since it requires the converging flow and thus the hard X-ray production region to be very close to the BH. However, no hard X-ray eclipse or any significant hard X-ray orbital modulation is seen in the BATSE or OSSE data.

6.3. Origin of the Short-Term Intensity Variations

Short-term variability was detected for the first time from a Galactic superluminal jet source in a high state. In view of the low (or no) variability in the 20–100 keV band, there are at least two possibilities to account for the detected short-term variability in the 1–10 keV band. One is that the ultrasoft component is variable. We consider this to be unlikely since no similar variability is seen from the ultrasoft component of other BHBs, unless the nature of this ultrasoft component is different owing to the jet ejection nature of this system. (However, the energy spectrum does not look different from other BHBs.) Two other BHCs, namely GX 339-4 (Miyamoto et al. 1991) and GS 1124–68 (Miyamoto et al. 1991, 1994; Ebisawa et al. 1994), in their high state have been detected with a combination of strong hard X-ray power-law tails and moderate ($\sim 5\%$) rms variations. These variations were found to be related to the power-law tails, and such a power-law-like PDS from GRO J1655–40 was not seen from them.

The other possibility is that the power-law component is variable but that the variability has an energy dependency so that the 1–10 keV power law is significantly variable but the 20–100 keV power law is not. To account for the 5.5% variability with only about 25% of the 1–10 keV flux in the power-law component, the intrinsic variability in the 1–10 keV power-law component has to be as high as 20%. Energy-dependent variations have been observed previously from other BHBs (Ebisawa et al. 1994; Miyamoto et al. 1991). The combined 1–10 keV variability and 20–100

keV low (or no) variability is, however, unusual among BHBs.

Between the hard X-ray outbursts, almost identical short-term variability has also been observed by *ASCA* from GRO J1655–40 and GRS 1915+105 (Ebisawa et al. 1997). GRS 1915+105 is the only other detected Galactic superluminal jet source. Its energy spectrum (power-law with cutoff above 5 keV, plus Fe-K absorption feature) is significantly different from the two-component spectrum we presented here. This strongly suggests that *this kind of short-term variability is related not to a specific energy spectral component but to the property that these systems can produce superluminal jets.* This variability is, however, not directly related to the presence of jets because of the lack of significant radio emission during these observations.

7. SUMMARY

The broadband high-energy observations presented here have for the first time detected a two-component energy spectrum and short-term variability in the 1–10 keV band from a superluminal jet source. The former is shared by all types of identified BHBs but not by any known neutron star system, and it is therefore a firm signature from BHBs. The latter is unusual among BHBs and is probably somehow related to the uniqueness of this source as a superluminal jet BHB. We have constrained the mass of the central compact object and the binary system inclination angle using the X-ray energy spectrum combined with optical radial velocity measurements. Our results further support the system containing a black hole with the highest inclination angle of all known BHBs in our Galaxy. The origin of the hard X-ray power-law component is still uncertain. Thermal Comptonization is unlikely to be the hard X-ray production mechanism, in view of the rather steep and unbroken power law up to very high energies. Jet origin models also seem difficult owing to the apparent lack of significant radio emission during this and the previous hard X-ray outburst. The converging flow model seems consistent with the spectral data, but it requires the hard X-ray production region to be compact. This can be tested if this system is an X-ray-eclipsing BHB. The origin of the short-term variability in the 1–10 keV band is also puzzling. This is perhaps related to the unique nature of this source as a superluminal jet BHB.

We appreciate the supports of the *ASCA*, BATSE, and WATCH teams for data collection and analysis. We also thank Jan van Paradijs and Craig Robinson for many interesting discussions. Finally, we are very grateful to the referee, R. M. Hjellming, for comments and suggestions, which certainly improved this article.

REFERENCES

- Alexandrovich, N., Borozdin, K., Efremov, V., & Sunyaev, R. 1994, IAU Circ. 6087
 Alexandrovich, N., Borozdin, K., & Sunyaev, R. 1995, IAU Circ. 6143
 Bailyn, C. D., et al. 1995a, *Nature*, 374, 701
 ———, 1995b, *Nature*, 378, 157
 Brandt, W. N., Podsiadlowski, Ph., & Sigurdsson, S. 1995, *MNRAS*, 277, L35
 Chakrabarti, S. K., & Titarchuk, L. 1995, *ApJ* 455, 623
 Cray, D., et al. 1996, *ApJ* 463, 79
 Ebisawa, K., et al. 1994, *PASJ*, 46, 375
 ———, 1997, in preparation
 Fishman, G. J., et al. 1989, in *Gamma Ray Observatory Science Workshop*, ed. C. R. Shrader, N. Gehrels, & B. Dennis (Greenbelt: NASA), 2-39
 Harmon, B. A., et al. 1992, in *AIP Conf. Proc. 280, Compton Gamma Ray Observatory*, ed. M. Friedlander, N. Gehrels, & D. J. Macomb (New York: AIP), 314
 ———, 1995, *Nature*, 374, 703
 Hjellming, R. M. 1996, in *ASP Conf. Proc., IAU Colloq. 163*, ed. D. T. Wickramasinghe, L. Ferrario, & G. V. Bicknell, in press
 Hjellming, R. M., & Rupen, M. P. 1995, *Nature*, 375, 464
 Israel, G. L., Mereghetti, S., & Stella, L. 1993, IAU Circ. 5889

- Kroeger, R. A., et al. 1996, A&AS, in press
 Levinson, A., & Blandford, R. 1996, ApJ, 456, L29
 Lund, N. 1986, in X-Ray Instrumentation in Astronomy, ed. J. L. Culhane (Proc. SPIE Int. Soc. Opt. Eng. 597), 95
 Makishima, K., et al. 1986, ApJ, 308, 635
 Margon, B. 1988, ARA&A, 22, 507
 Mereghetti, S., Stella, L., & De Nile, F. 1993, A&A, 278, L23
 Mirabel, I. F., & Rodríguez, L. F. 1994, Nature, 371, 46
 Mitsuda, K., et al. 1984, PASJ, 36, 741
 Miyamoto, S., et al. 1991, ApJ, 383, 784
 ———. 1994, ApJ, 453, 398
 Sazonov, S. Y., Sunyaev, R. A., & Lund, N. 1996, in Röntgenstrahlung from the Universe, ed. H. U. Zimmermann, J. Truemper, & H. W. Yorke (MPE Report 263) (Garching: Max-Planck-Institut fuer Extraterrestrische Physik), 187
 Shakura, N. I., & Sunyaev, R. A. 1973, A&A, 4, 337
 ———. 1976, MNRAS, 175, 613
 Shu, F. H. 1991, The Physics of Astrophysics (Mill Valley: University Science Books)
 Shimura, T., & Takahara, F. 1995, ApJ, 445, 780
 Strom, R. G., et al. 1989, Nature, 337, 234
 Sunyaev, R., et al. 1988, Astron. Lett., 14, 771
 Sunyaev, R., et al. 1994, Astron. Lett., 20, 890
 ———. 1997, in preparation
 Tanaka, Y., Inoue, H., & Holt, S. S. 1994, PASJ, 46, L37
 Tanaka, Y., & Lewin, W. H. G. 1995, in X-ray Binaries, ed. W. H. G. Lewin, J. van Paradijs, & E. van den Heuvel (Cambridge: Cambridge Univ. Press), 126
 Tingay, S. J., et al. 1995, Nature, 374, 141
 Ueda, Y., et al. 1997, in preparation
 White, N. E. 1993, in AIP Conf. Proc. 308, The Evolution of X-Ray Binaries, ed. S. S. Holt & C. S. Day (New York: AIP), 53
 van der Hooft, F., et al. 1996, MNRAS, submitted
 van der Klis, M. 1994, ApJS, 92, 511
 van der Klis, M., & van Paradijs, J. 1994, A&A, 281, L17
 Zhang, S. N., Fishman, G. J., Harmon, B. A., & Paciesas, W. S. 1993, Nature, 366, 245
 Zhang, S. N., et al. 1994a, IAU Circ. 6046
 ———. 1994b, IEEE Trans. NS 41, 1313
 ———. 1995a, IAU Circ. 6209
 ———. 1995b, Exp. Astron., 6, 57
 ———. 1996, A&AS, in press
 ———. 1997, in preparation

Note added in proof.—After the acceptance of this article for publication, we became aware of new results obtained by C. D. Orosz and J. Bailyn (ApJ, in press [1997]) from optical light curve modeling of GRO J1655–40. Their mass value ($7.02 \pm 0.22 M_{\odot}$) and the binary inclination angle ($69^{\circ}50 \pm 0^{\circ}08$) are significantly different from what we obtained by combining the X-ray energy spectrum and the optical mass function. The apparent discrepancy might be caused by any of several factors. For example, if the black hole is rotating in the same direction as the accretion disk, the curves in our Figure 4 would all move upward, which implies a higher black hole mass for a given inclination angle. Applying the inferred black hole mass value and the inclination angle from Orosz and Bailyn to our X-ray M - i relationship and assuming the black hole has nonzero angular momentum (*Kerr* black hole), we obtain an inner disk radius of $\sim 2GM/c^2$, to be compared with $6GM/c^2$ for a *Schwarzschild* (*nonrotating*) black hole. This inner disk radius would correspond to the last stable orbit of a $\sim 95\%$ maximally rotating black hole. Also, the X-ray spectral model we used may not be sufficiently accurate when the inclination angle is very high and the inner disk boundary is very close to the horizon of the black hole.

